ELSEVIER

International Journal of Mass Spectrometry 195/196 (2000) 467–479

International Journal of Mass Spectrometry

Refining the model for selective cleavage at acidic residues in arginine-containing protonated peptides

George Tsaprailis, Árpád Somogyi, Eugene N. Nikolaev[1], Vicki H. Wysocki*

Department of Chemistry, University of Arizona, P.O. Box 210041, Tucson, AZ 85721-0041, USA

Received 10 June 1999; accepted 10 September 1999

Abstract

Simple glycine-based peptides containing acidic [aspartic (D) and glutamic acid (E)] and basic residues [arginine (R)] were dissociated by surface-induced dissociation (SID) both in a tandem double quadrupole (Q_1Q_2) and a hybrid sector/time-of-flight (TOF) mass spectrometer, as well as by low-energy collision-induced dissociation in an ion trap mass spectrometer. The synthetic peptides investigated were GDGGGDG, GDGGGDG**R,** **R**GDGGGDG, **R**GDGGGDG**R**, GGGDG**R**, GGGEG**R**, and GDGGGEG**R**. The mass spectral results obtained support and extend our previous findings that selective cleavages at the C–(O)–N bond adjacent to the acidic residues (C-side) predominate in the spectra when the number of ionizing protons equals or is less than the number of arginine residues. They also support our conclusion that these cleavages are induced by the side-chain acidic hydrogens of D or E residues. Stochastic molecular modeling procedures have been employed in this work to probe the gas-phase conformations for these protonated peptides. These searches have revealed possible conformers of singly protonated GGGDGR, and RGDGGGDG peptide ions where the protonated arginine is solvated by nearby carboxylic and carbonyl oxygens along with simultaneous intramolecular H bonding between the D side-chain acidic hydrogen(s) and the adjacent C-side peptide bonds. Electrospray ionization/surface-induced dissociation fragmentation efficiency curves (percent fragmentation versus SID laboratory collision energy) are also presented for some of these peptides. The relative position of these curves both with the Q_1Q_2 and sector/TOF instruments along with less pronounced selective cleavages for the E-containing peptides support our previous conclusion that selective cleavage at E residues require longer time frames for dissociation than for D-containing peptides. The total sum of these findings underscores the idea that gas-phase secondary structure (i.e. conformation) can have an influence in peptide fragmentation. (Int J Mass Spectrom 195/196 (2000) 467–479)

Keywords: Conformation; Peptides; Fragmentation; Enhanced cleavages; SID; CID; Aspartic Acid; Arginine

1. Introduction

Over the last two decades mass spectrometry has grown from a relatively underutilized resource to one that is now used routinely in analytical, biochemical, immunochemical and medicinal research or service facilities [1]. This is largely due to the development of "soft" ionization methods such as matrix-assisted

* Corresponding author. E-mail: vwysocki@u.arizona.edu

[1] On leave from the Institute of Energy Problems of Chemical Physics, Moscow, Russia.

Dedicated to Bob Squires for his many seminal contributions to mass spectrometry and ion chemistry.

1387-3806/00/$20.00
PII S1387-3806(99)00221-3

laser desorption ionization (MALDI) [2], and electrospray ionization (ESI) [3–5], which allow formation of singly or multiply charged biomolecules such as peptides and proteins. In fact, due to the recent increase in demand for sequencing of peptides as well as identification of proteins by mass spectrometry, several computer sequencing programs now exist which rely on mass spectrometry and tandem mass spectrometry (MS/MS) data [6–11].

Although MS/MS is an important tool for protein and peptide characterization, it has been found that differences exist in fragmentation efficiencies and in specific fragmentation patterns for different peptides which can often hinder characterization of a peptide's complete structure. These differences are often controlled by various structural parameters [12–27] and include the nature of the residues present (neutral versus acidic versus basic) [15,28–31], the charge state of the precursor ion [16,17,23], the composition of the peptide backbone (e.g. N-alkylated) [18], and the size [32,33]. The notion of protonated peptides in the gas-phase adopting similar conformations that can subsequently affect their dissociation behavior is yet another of these control factors currently being investigated by various researchers [34–44].

Recently we have shown that collisional dissociation of protonated peptide ions containing arginine (R) and aspartic or glutamic acid (D/E) residues result in selective cleavages at the acidic residues if the number of ionizing protons does not exceed the number of arginine residues [44]. To rationalize these findings, a model based on solvation of the "sequestered" charge on the R side chain by nearby carboxylic acid groups and preferential cleavage initiated by acidic hydrogens not involved in the charge solvation was proposed.

In the work presented here, we extend our previous investigations by examining the dissociation behavior of simple glycine-rich peptides containing R, D, and E residues. This was done to eliminate any side-chain–side-chain interactions between neighboring residues which might be affecting fragmentation in the peptides investigated earlier [44]. The peptides have been dissociated using surface-induced dissociation (SID) [45,46] in a tandem quadrupole mass spectrometer (Q_1Q_2) and in a novel hybrid sector/time-of-flight (TOF) mass spectrometer [47] and by low-energy collision-induced dissociation (CID) [5,48] in an ion trap (IT) mass spectrometer. In addition, stochastic molecular dynamics calculations have been carried out on some of these peptides to see if the singly protonated ions can adopt conformations that can support our previous model derived from experimental mass spectral data.

2. Experimental

2.1. Peptide synthesis

The synthetic peptides used were prepared using multiple solid-phase synthesis protocols outlined by Atherton and Sheppard [49]. 9-Fluoroenylmethoxycarbonyl (Fmoc) derivatives of the various amino acids required [Fmoc-L-arginine, 2,2,5,7,8-pentamethlchroman-6-sulfonyl (Pmc); Fmoc-L-glutamic acid, *t*-butyl; Fmoc-L-aspartic acid, *t*-butyl; Fmoc-L-glycine] were purchased from Advanced Chemtech (Louisville, KY). The C-terminal residues required for peptide synthesis were purchased already attached to resins from Calbiochem/Novabiochem (San Diego, CA). All other reagents required during synthesis were from Aldrich (Milwaukee, WI). The following peptides were synthesized: GGGDGR, GDGGGDGR, RGDGGGDG, RGDGGGDGR, GDGGGDG, GGGEGR, and GDGGGEGR.

2.2. Surface-induced dissociation in a quadrupole tandem mass spectrometer

The instrument used for these experiments is a quadrupole tandem mass spectrometer (Q_1Q_2) specifically designed for low-energy ion-surface collisions and has been previously described [16,27,46]. Peptide analytes were dissolved in a 70/30% (v/v) mixture of methanol/H_2O containing 1% acetic acid to give the appropriate concentration (~30–50 pmol/μL), and sprayed at atmospheric pressure from a syringe needle held at 4.2–4.7 kV (flow rate of 2 μL/min), toward a metal capillary (120 V). The temperature of the metal capillary was maintained at 120 °C to ensure proper desolvation of the ions. The desolvated ions were directed toward a skim-

mer cone (90 V), after which they entered into the high-vacuum region of the mass spectrometer, where they were analyzed and detected. Fragmentation efficiency curves, Σ (fragment ion signal intensities)/[(parent ion signal intensity) + Σ (fragment ion signal intensities)] versus collision energy, were plotted by fitting a logistic curve to the data points. The SID (laboratory) collision energy was controlled by the potential difference between the ion source skimmer cone and the surface [16]. SID mass spectra were obtained over a range of collision energies, and the fragmentation efficiency curves reported here represent the average of a minimum of two data sets. The chemically modified surface used in the SID experiments was a self-assembled monolayer film of octadecanethiol or 2-(perfluorodecyl)ethanethiol on gold [50]. Gold surfaces (1000 Å of vapor-deposited gold on silica) were obtained from Evaporated Metal Films (Ithaca, NY) and cleaned by using a UV cleaner (UV-Clean, Boekel, Philadelphia, PA) before immersion into the alkanethiol solution (1 mM ethanol, 24 h) as previously described [16].

2.3. Collision-induced dissociation in an ion trap (LCQ) mass spectrometer

The peptides were dissolved in a solution of H_2O:MeOH (1:1; v/v) containing 1% acetic acid to make up a concentration of 20–30 pmol/μL. The peptide solutions were then sprayed into the Finnigan LCQ mass spectrometer (San Jose, CA) at a rate of 3 μL/min. The applied needle voltage used was 4.8 kV and the capillary temperature was maintained at 200 °C for all samples. Unit mass selection of the precursor ion was performed in order to avoid ambiguities from isotope contributions. The excitation energy (indicated as % collision energy by the manufacturer), was incremented in small steps to selectively monitor low energy fragmentation processes for the precursor ions selected.

2.4. Surface-induced dissociation in a hybrid sector/time-of-flight mass spectrometer

A JEOL HX 110A sector (E/B) instrument (JEOL, U.S.A.) was modified by the "in-line" addition of a TOF set up with a quadratic accelerator to perform SID experiments. The instrument design is described elsewhere [47]. Singly charged precursor ions were generated by the fast-atom bombardment (FAB) source of the sector instrument (Xe gun; glycerol:thioglycerol:meta-nitrobenzyl alcohol = 2:1:1 matrix containing 1% trifluoroacetic acid). Collision energies ranged from 10 to 50 eV and dissociation times were on the order of 0.1–30 μs.

2.5. Molecular modeling

The peptides GGGDGR, and RGDGGGDG were built in MACROMODEL [51] (Version 6.0) by using the program's amino acid library. They were then modified to carry one positive charge with the charge being placed on the arginine residue side chain. The built-in protonated peptide structures were first subjected to 500 optimization iterations in MACROMODEL resulting in an energetically refined starting structure. Stochastic molecular dynamics using the AMBER forcefield [52] were then performed on each of these structures using the Batchmin program of Macromodel. AMBER forcefield default parameters were used for the electrostatic and hydrogen bonding treatments during the molecular dynamics. Moreover, large distance cut off values were assigned to ensure smoother convergence and the Polak-Riviere Conjugate Gradient (RPCG) [53] was used for the program's energy minimization routines. In all, 10 000 structures were sampled during the stochastic dynamics run (1 fs time step; 10 000 ps total time; 800 K initial and final temperature; 0.5 ps bath time). Our choice of temperature for the molecular dynamics was based on previous analysis of kinetic energy transfer into internal energy for singly protonated YGGFL using thermal decomposition kinetics methods [54]. Those results showed that applying the thermal kinetic parameters to the dissociation rate constant for singly protonated YGGFL at the inflection point of the SID fragmentation efficiency curve yields an effective temperature of 796 K.

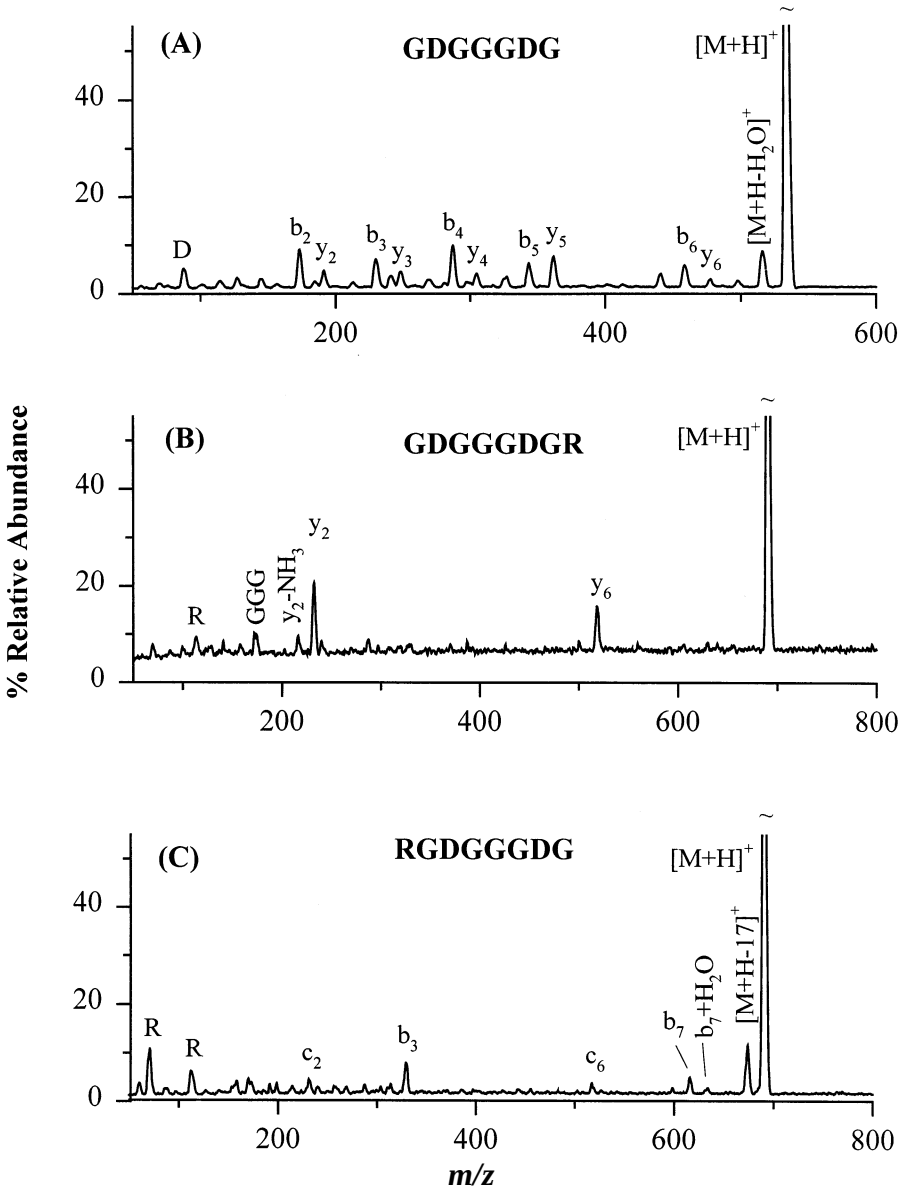

Fig. 1. ESI/SID spectra of (A) singly protonated GDGGGDG at a collision energy of 17.5 eV, (B) singly protonated GDGGGDGR at a collision energy of 32.5 eV, and (C) singly protonated RGDGGGDG at a collision energy of 35 eV. In all cases a 2-(perfluorodecyl)ethanethiolate ($CF_3(CF_2)_9CH_2CH_2SAu$) monolayer surface was used in the Q_1Q_2 mass spectrometer.

3. Results and discussion

3.1. Selective cleavage at acidic residues when the number of ionizing protons does not exceed the number of arginine residues

Fig. 1(A) shows the product ion mass spectrum of singly protonated GDGGGDG obtained by SID in a tandem quadrupole instrument. The spectrum is rich in sequence information as evidenced by abundant b_n and y_n ions indicative of indiscriminant cleavage along the peptide backbone. Introduction of an R residue on the C- or N-terminal end of this simple peptide to generate GDGGGDGR [Fig. 1(B)] and RGDGGGDG [Fig. 1(C)], respectively, results in

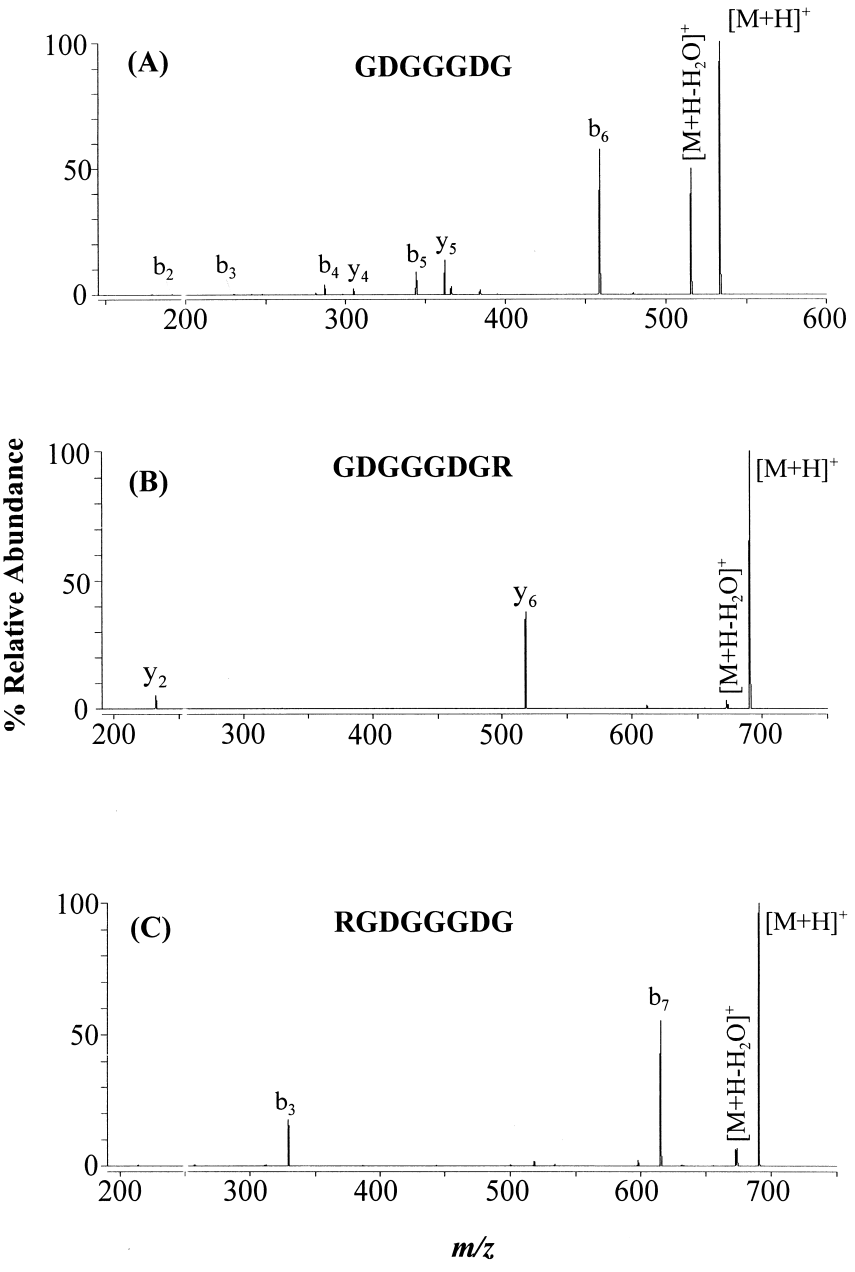

Fig. 2. Low-energy ESI/CID spectra of (A) singly protonated G<u>D</u>GGG<u>D</u>G at a 13.5% relative collision energy, (B) singly protonated G<u>D</u>GGG<u>D</u>GR at a 20% relative collision energy, and (C) singly protonated RG<u>D</u>GGG<u>D</u>G at a 19.5% relative collision energy in the Finnigan IT mass spectrometer; collision gas is He. Dominant b_{n-1} fragment ions (b_6 in singly protonated G<u>D</u>GGG<u>D</u>G) are relatively common in nonbasic peptides [58].

significant changes to the product ion mass spectra of the singly protonated precursor ions, $[M + H]^+$. Selective and enhanced cleavages adjacent to D residues (C-side) are observed across the whole range of collision energies investigated (25–45 eV). Specifically, predominant y_2 and y_6 product ions are ob-

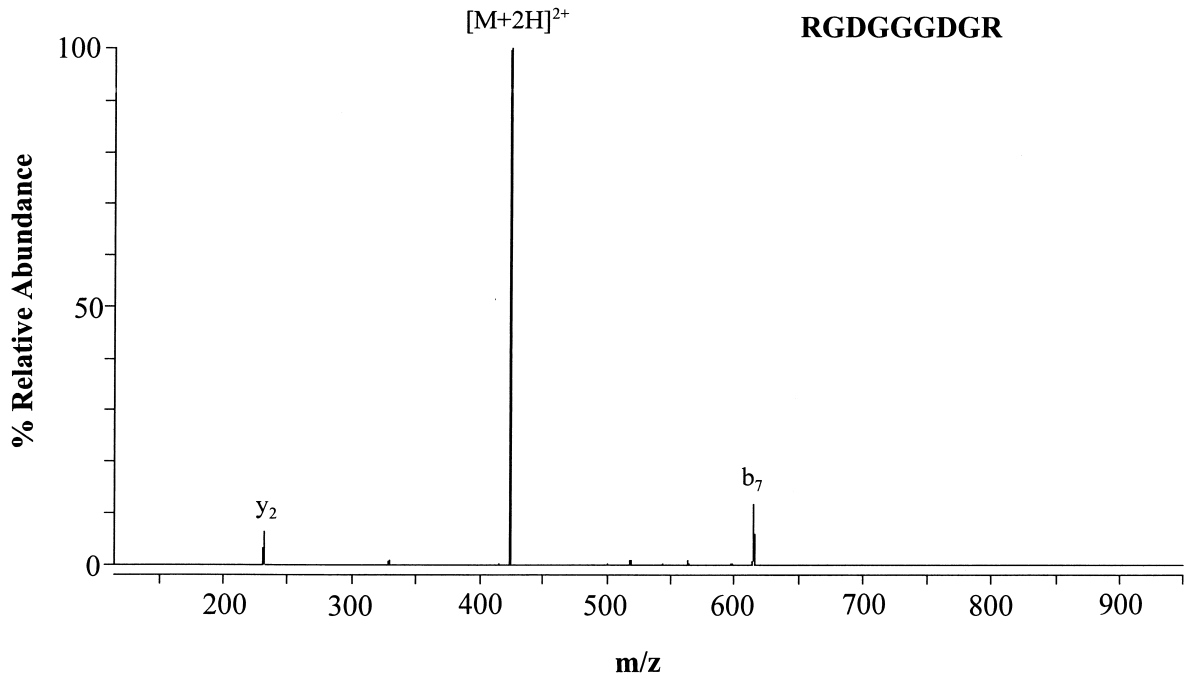

Fig. 3. ESI/CID spectra of doubly protonated RGDGGGDGR at a 11% relative collision energy. IT mass spectrometer; collision gas is He.

served for GDGGGDGR, whereas strong b_3 and b_7 product ions are seen for RGDGGGDG [Fig. 1(B) and (C), respectively). These predominant *b*- and *y*-type ions are due to cleavages at the second and sixth residues (D) in GDGGGDGR, and the third and seventh residues (D) in RGDGGGDG. Very similar results were obtained using low energy ESI/CID in the IT (Fig. 2).

These results mirror our previous observations where we found enhanced cleavages at the C-terminal C–(O)–N bond adjacent to D residues dominating the MS/MS spectra of $[M + H]^+$ ions of LDIFSDFR and RLDIFSDF irrespective of the activation method (SID or CID) employed [44]. In contrast, the MS/MS spectra [ESI/SID or ESI/CID; Figs. 1(A) and 2(A), respectively] of D-containing peptides devoid of any R residues (e.g. GDGGGDG), do not show any selective or enhanced cleavages. This lack of enhanced cleavage at D residues when the protonated R is absent is similar to reports for the $[M + H]^+$ ions of LDIFSDF. Such reproducibility in results reported on the selective cleavage at D residues only in the presence of R residues highlights the need for a very basic residue (i.e. arginine) or a strongly held charge [55].

Fig. 3 shows the product ion spectrum of $[M + 2H]^{2+}$ ions of RGDGGGDGR obtained by low-energy ESI/CID (11% relative collision energy) in the IT instrument. The striking similarity between this spectrum and those previously reported for the $[M + 2H]^{2+}$ ions of RLDIFSDFR by using SID and sustained off-resonance irradiation (SORI) CID [44], showing selective cleavage at the D in the seventh position, indicate side-chain–side-chain interactions (other than R–D) do not play a role in the dissociation.

3.2. Kinetic control of diagnostic cleavages at aspartic versus glutamic acid residues

Fig. 4 shows the ESI/SID fragmentation efficiency curves of the $[M + H]^+$ ions of GGGDGR, GGGEGR, GDGGGDGR and GDGGGEGR on the Q_1Q_2 mass spectrometer. Similar SID fragmentation efficiency curves were obtained for the singly proto-

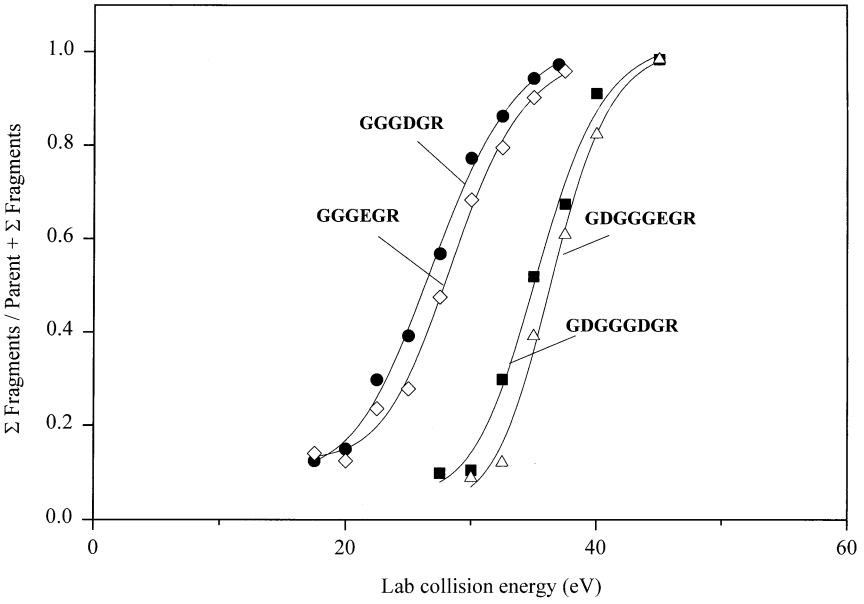

Fig. 4. ESI/SID fragmentation efficiency curves of the $[M + H]^+$ ions of GGGDGR (circle), GGGEGR (diamond), GDGGGDGR (square) and GDGGGEGR (triangle) obtained with the Q_1Q_2 mass spectrometer. The *y* axis represents the ratio of Σ (fragment ion signal abundance)/Σ (parent ion signal abundance) + Σ (fragment ion signal abundance) and the *x*-axis represents the SID (laboratory) collision energy (eV). The ESI/SID spectra used to prepare the fragmentation efficiency curves were obtained by collision of the $[M + H]^+$ ions with a surface prepared from 2-(perfluorodecyl)ethanethiolate $[CF_3(CF_2)_9CH_2CH_2SAu]$ on vapor deposited gold.

nated precursors of GGGDGR and GGGEGR on the hybrid sector-TOF instrument (data not shown). A decrease in the fragmentation efficiency (curves shifted to higher SID energies) is observed for the peptides incorporating an E residue. This shift in energy is similar to, although not as large, as that reported earlier for the $[M + 2H]^{2+}$ ion species of RLDIFSDFR and RLEIFSEFR [44]. Moreover, this clear trend is reproducible within sample sets (i.e. GGGDGR and GGGEGR or GDGGGDGR and GDGGGEGR), and between instrumental setups implying that more energy is required for efficient dissociation of the E-containing peptides. The MS/MS spectral data for the $[M + H]^+$ ions of GGGEGR following SID show that the selective cleavage at E residues is less pronounced at any one given energy than that for GGGDGR [3% of total relative abundance versus 13%, respectively; Fig. 5(A) and (B)]. This holds true at all the collision energies investigated and might explain the fragmentation efficiency shifts seen in Fig. 4. Similarly, the SID spectra of singly protonated GDGGGDGR [Fig. 1(B)] are different from those obtained for GDGGGEGR with respect to the dominance of cleavage at the second acidic residue site (D or E at position six). The y_2 product ion corresponding to cleavage of the EG amide bond of GDGGGEGR (spectra not shown) is consistently less abundant than that for GDGGGDGR by SID. No great distinction in intensities, however, between peptides (GGGDGR/GGGEGR or GDGGGDGR/GDGGGEGR) is observed for the y_2 product ions following dissociation by low-energy CID in the IT [the former set of peptides is shown in Fig. 5(E) and (F)]. We have previously observed dominant and preferred cleavage adjacent to the E residue at position seven in doubly protonated RLEIFSEFR by IT and SORI-CID but not by SID [44]. Our current observations on the dissociation of singly protonated GGGEGR in the IT mirrors these findings. A similar argument based on kinetic control can be made for the selective cleavages at D and E residues observed for fibrinopeptide A (ADSGEGD

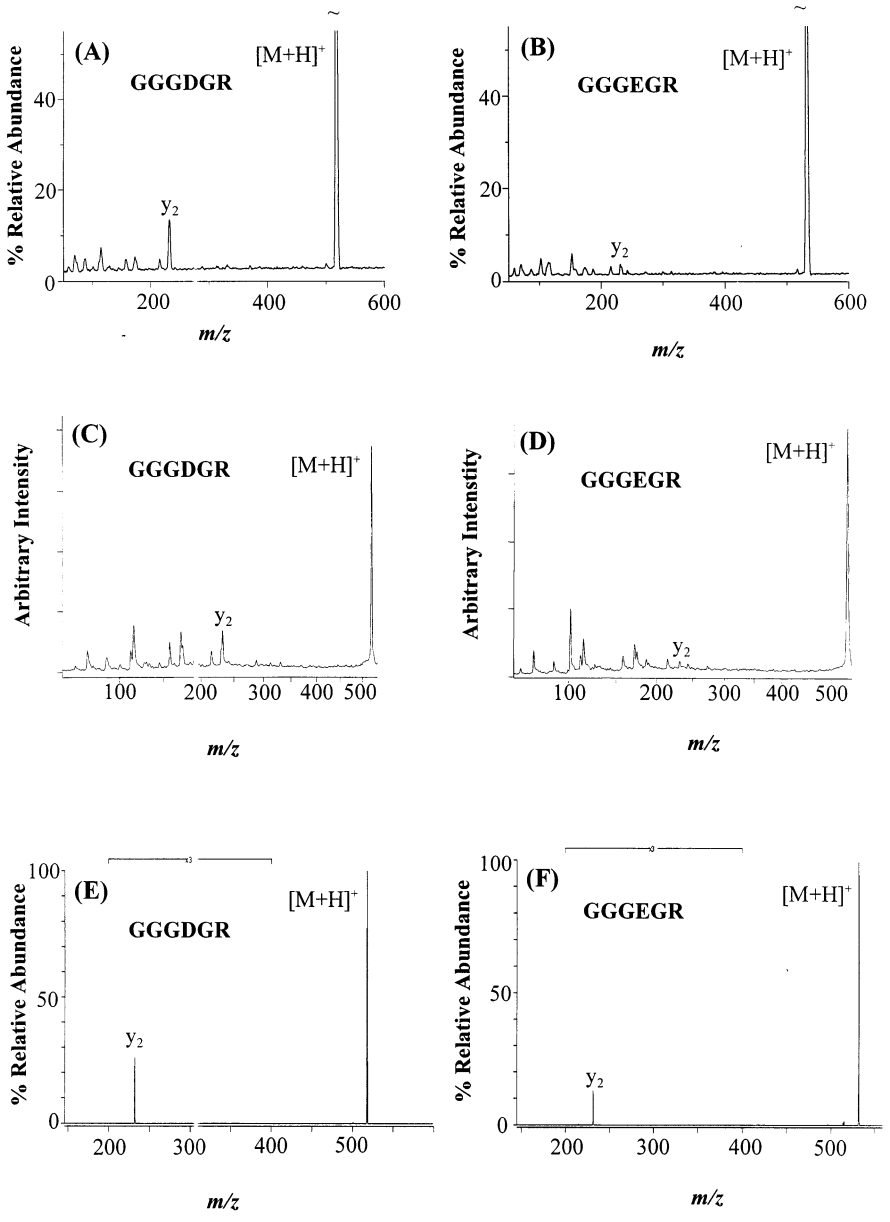

Fig. 5. ESI/SID spectra of (A) singly protonated GGGDGR at a collision energy of 22.5 eV and (B) singly protonated GGGEGR at a collision energy of 22.5 eV on a 2-(perfluorodecyl)ethanethiolate ($CF_3(CF_2)_9CH_2CH_2SAu$) monolayer surface. Q_1Q_2 mass spectrometer. SID spectra obtained in the hybrid sector/TOF mass spectrometer for (C) singly protonated GGGDGR and (D) singly protonated GGGEGR. Low-energy ESI/CID spectra of (E) singly protonated GGGDGR and (F) singly protonated GGGEGR both at a 15% relative collision energy in the Finnigan IT instrument.

FLAEGGGVR) by SORI-CID with the intensity ratios $(y_5 + y_{11}) < (y_9 + y_{14})$ (Fig. 6). Note that by SID, only predominant cleavages at D residues are observed (data not shown).

3.3. Molecular modeling

Following the stochastic molecular dynamics routine, the 10 000 annealed structures of singly proto-

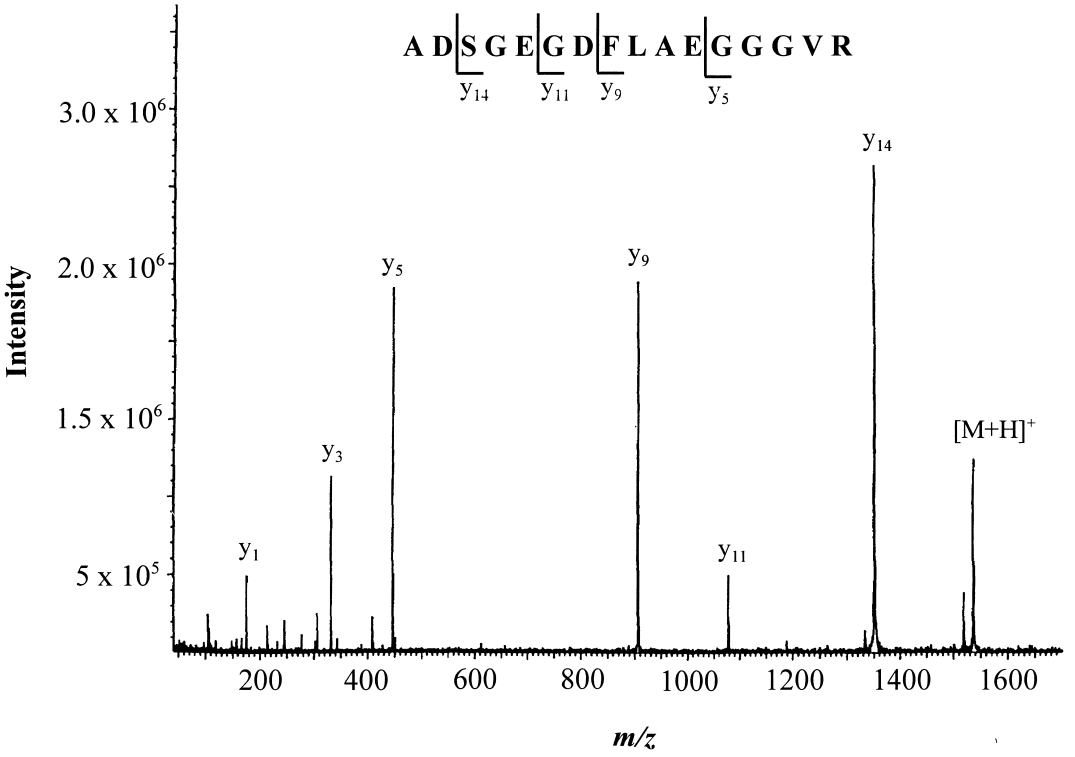

Fig. 6. SORI mass spectrum in a Fourier tandem mass spectrometer of singly protonated fibrinopeptide A at an excitation energy of 45.7 eV; Bruker Fourier transform mass spectrometer; CO_2 collision gas; electrospray ionization.

nated GGGDGR and RGDGGGDG were put through a filtering process to identify subsets of conformations that contained hydrogen bonds (cutoff distance of 2.5 Å) between specific donor and acceptor groups. The groups considered included the protonated guanidino side chain of arginine, the peptide bond heteroatoms as well as the carboxylate groups of the C-terminus and aspartic acid side chain(s). It was found that in ~5% of all structures of singly protonated RGDGGGDG, the protonated R side chain was solvated by carboxylate groups and/or peptide carbonyls, and simultaneously the free acidic hydrogens of D residues were within H-bonding distance to their C-side amide bonds. Previously [44] we had proposed that the enhanced cleavages at the acidic residues in R-containing protonated peptides (in the cases where the number of ionizing protons does not exceed the number of R residues), are induced by the acidic carboxylate hydrogens not involved in solvating the protonated R side chain (see Scheme 1 discussed later). With this in mind, several representative structures of RGDGGGDG which support this dissociation model are shown in Fig. 7. Fig. 7(A) depicts a molecule where the two termini solvate each other (i.e. N-terminal protonated R side chain H bonds to the C-terminal carboxyl oxygen). In addition, the D residue at position seven is within H-bonding distance to the seventh carbonyl oxygen. Subsequent formation of a five-membered ring involving the carbonyl carbon along with proton transfer to the amide nitrogen (which has been shown to weaken the amide bond), can lead to a fragmenting structure [see dashed line in Fig. 7(A)]. Such a conformer can be used to rationalize the b_7 product ion seen in the MS/MS spectra of singly protonated RGDGGGDG [Figs. 1(C) and 2(C)]. Based on this structure, potential energy surface calculations are planned to probe the interaction of the peptide carbonyl oxygen and the acidic

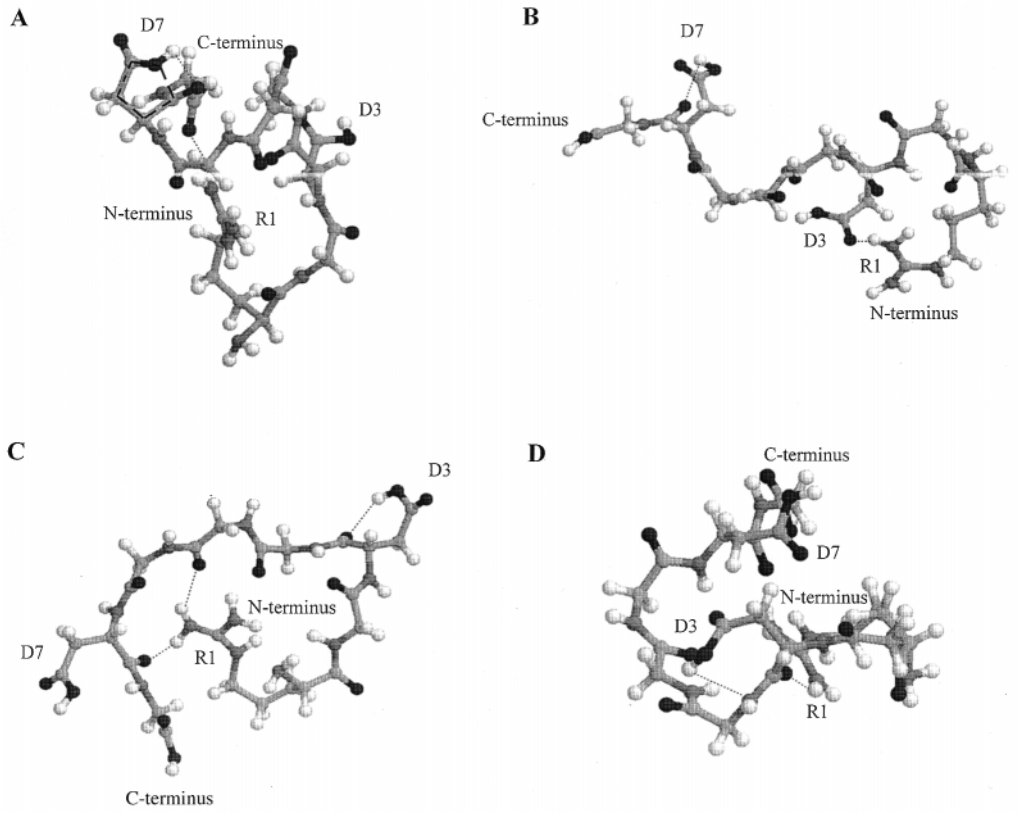

Fig. 7. Molecular dynamics simulation structures at 800 K of singly protonated RGDGGGDG showing (A) the interaction between protonated R and C-terminus and the H-bonding between D7 and its C-terminal peptide bond, (B) the interaction between protonated R and D3 and the H-bonding between D7 and its C-terminal peptide bond, (C) the multiple interactions of protonated R to carbonyl oxygens and the H-bonding between D3 and its C-terminal peptide bond, and (D) the interaction between protonated R and the third carbonyl peptide oxygen as well as the H-bonding between D3 and its C-terminal amide nitrogen. H-bonding interactions are represented by the dotted lines. The dashed line in (A) is meant to draw attention to the five-membered ring structure described in the text.

hydrogen of the D residue similar to that shown in Fig. 7(A).

In Fig. 7(B) we see a conformer where the protonated R side chain is solvated by the D residue at position three. The D residue at position seven not involved in any solvation processes can induce cleavage C-terminal to it as described above. It should be noted that solvation of the protonated R side chain by the D residue at position three ties up the side chain of R in this structure preempting other H-bonding interactions so cleavage at position three is less likely.

In many of the structures sampled, the protonated guanidino side chain of R is H bonded to one or more peptide carbonyl oxygens. In addition, conformers exist where both hydrogens on the nitrogen bearing the charge are solvated simultaneously. Based on collision cross section measurement, a highly solvated system for bradykinin (RPPGFSPFR) up to 600 K has been proposed by Wyttenbach et al. and involves wrapping of the molecule around the charge center(s) [36]. Fig. 7(C) shows a structure of RGDGGGDG where the R side-chain is solvated by the fifth and seventh peptide carbonyl oxygens allowing the D residue at position three to induce cleavage [b_3 fragment ion in Figs. 1(C) and 2(C)]. It is of interest that no structures were found where both D residues are simultaneously within H-bond distance to their respective amide bonds.

A rather interesting H-bonding trend is noted in

Fig. 7(D) and involves the acidic residue side chain carboxylate hydrogen and its C-side adjacent amide nitrogen along with concomitant H bonding between protonated R and the D backbone carbonyl oxygen. N protonation of the amide nitrogen leading to weakening of the peptide bond has been previously reported by Somogyi et al. [56] whereas H bonding to the carbonyl oxygen strengthens it. The molecular dynamics results indicate that no one specific structure for protonated RGDGGGDG predominates and that multiple conformers may exist. Similar results were obtained for singly protonated GGGDGR with the exception that a smaller percent of structures (~1%) contained similar interactions as those discussed for RGDGGGDG above. This is not surprising since it is expected that fragmenting structures (following deposition of energy in a mass spectrometer), would not represent the major population of stable structures. No interaction of the side-chain acidic hydrogen to the C-terminal amide nitrogen, however, was found.

Scheme 1 illustrates a model (presented in our previous publication [44] and essentially an extended version of that of Yu et al. [57], for two of the peptides investigated which rationalizes the enhanced cleavages at acidic residues. Scheme 1(A) shows the interactions in singly protonated GDGGGDGR leading to the specific cleavages at the second and sixth D residue [i.e. y_2 and y_6 in Figs. 1(B) and 2(B)]. Similar intramolecular interactions can be envisioned for singly protonated GDGGGEGR, GGGDGR, and GGGEGR. We speculate that for the $[M + 2H]^{2+}$ ions of RGDGGGDGR (Fig. 3), one of the charges is solvated between the guanidino side-chain of the N-terminal R residue and the acidic side chain of the D residue at the third position, respectively, whereas the C-terminal protonated R residue is solvated by the carboxy terminus [Scheme 1(B)]. This would allow the acidic proton on the D at the seventh position to intramolecularly induce fragmentation at its C-terminal amide bond leading to an enhanced cleavage [Scheme 1(B); y_2/b_7 in Fig. 3]. This model can also be used to rationalize the MS/MS results of fibrinopeptide A (ADSGEGDFLAEGGGVR) by SORI-CID shown in Fig. 6 (enhanced cleavage is seen at each of the two D and two E residues). Application of our

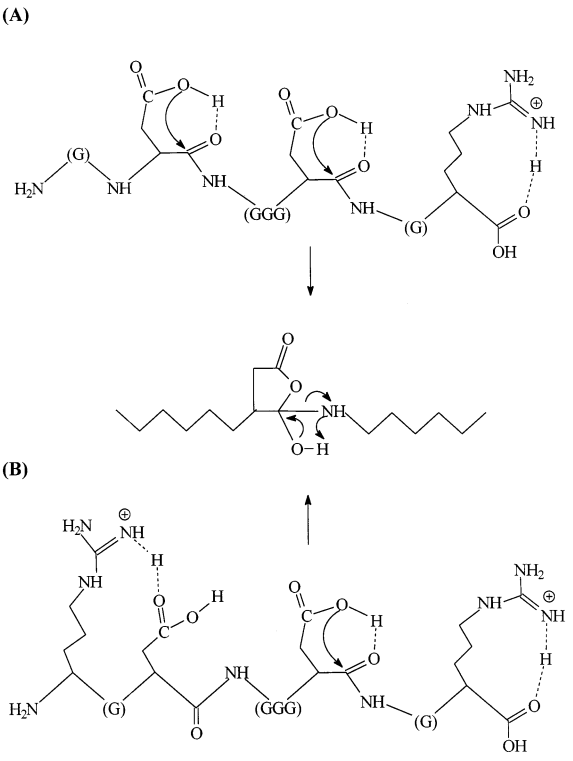

Scheme 1. Model illustrating the intramolecular interactions leading to the specific cleavages at (A) the second and sixth D residue in singly protonated GDGGGDGR and (B) the seventh D residue in doubly protonated RGDGGGDGR. Based on the modeling results, simultaneous cleavage at both D residues in singly protonated GDGGGDGR cannot occur. Moreover, the dashed lines are meant to indicate that H-bonding can occur to either the amide oxygen or nitrogen.

model to this peptide suggests that the selective cleavages are induced by the acidic hydrogens not solvating the protonated R residue in this peptide. Qin and Chait have also observed similar fragmentation (i.e. enhanced cleavage at each of the three D and three of the four E residues) for [Glu-1] fibrinopeptide B [30]. Recent data from our group on SID and CID of fixed-charge derivatives of D-containing peptides (e.g. LDIFSDF) lend further support that acidic hydrogen(s) on the side chain of D residues do initiate the cleavages; in the absence of added protons the selective cleavage adjacent to D residues still predominates the fragmentation spectra ([55] and unpublished results).

4. Conclusion

The mass spectral results presented on D (or E) and R-containing glycine-based peptides as well as the modeling results support selective cleavage at D and E acidic residues when the number of ionizing protons does not exceed the number of R residues. They also show that side-chain–side-chain interactions (other than those between R and D/E) are not important in explaining enhanced cleavages at these residues. Further, they support previous observations that selective cleavages at acidic residues predominate the mass spectra of arginine-containing peptides given a suitable sampling time frame. Of importance is the acidic hydrogen on D hydrogen bonded with the adjacent C-side carbonyl oxygen allowing for easy nucleophilic attack of the carboxylic oxygen on the carbonyl carbon of the C–(O)–N bond (C-side) to form a five membered ring and an ensuing proton transfer to the amide nitrogen that leads to breaking of the amide bond.

To date, only minor changes have been made to existing mass spectrometry-based sequencing algorithms to take into account the very striking cleavage pattern in peptides incorporating both acidic and several basic residues. It is hoped that mass spectrometry-based sequencing programs will incorporate this predictive rule of cleavage at acidic residues in the future.

Acknowledgements

This work was financially supported by a grant from the National Institutes of Health (GM RO151387 to V.H.W.), the National Science Foundation (NSF-ARI CHE-9601809 to V.H.W.) and a postdoctoral fellowship from the Fonds pour la Formation de Chercheurs et l'Aide à la Recherche (to G.T.). The authors wish to thank Wenqing Zhong for providing the fibrinopeptide A SORI-CID tandem mass spectrum and Linda Breci for help with the modeling analyses.

References

[1] A.R. Dongré, J.K. Eng, J.R. Yates III, Trends Biotech. 15 (1997) 418.
[2] F. Hillenkamp, J. Karas, R.C. Beavis, B.T. Chait, Anal. Chem. 63 (1991) 1193A.
[3] J.B. Fenn, M. Mann, C.K. Meng, S.F. Wong, C.M. Whitehouse, Mass Spectrom. Rev. 9 (1990) 37.
[4] R.D. Smith, J.A. Loo, C.G. Edmonds, C.J. Barinaga, H.R. Udseth, Anal. Chem. 62 (1990) 882.
[5] R.D. Smith, J.A. Loo, C.J. Barinaga, C.G. Edmonds, H.R. Udseth, J. Am. Soc. Mass Spectrom. 1 (1990) 53.
[6] J.K. Eng, A.L. McCormack, J.G. Yates III, J. Am. Soc. Mass Spectrom. 5 (1994) 976.
[7] J.R. Yates III, J.K. Eng, A.L. McCormack, D. Schieltz, Anal. Chem. 67 (1995) 1426.
[8] J.R. Yates III, J.K. Eng, A.L. McCormack, Anal. Chem. 67 (1995) 3202.
[9] M. Mann, M. Wilm, Anal. Chem. 66 (1994) 4390.
[10] R.S. Johnson, K. Biemann, Biomed. Environ. Mass Spectrom. 18 (1989) 945.
[11] W.M. Hines, A.M. Falick, A.L. Burlingame, B.W. Gibson, J. Am. Soc. Mass Spectrom. 3 (1992) 326.
[12] D.F. Hunt, J.R. Yates III, J. Shabanowitz, S. Winston, C.R. Hauer, Proc. Natl. Acad. Sci. USA 83 (1986) 6233.
[13] R.L. Winston, M.C. Fitzgerald, Mass Spectrom. Rev. 16 (1997) 165.
[14] K.D. Ballard, S.J. Gaskell, Int. J. Mass Spectrom. Ion Processes 111 (1991) 173.
[15] J.L. Jones, A.R. Dongré, Á. Somogyi, V.H. Wysocki, J. Am. Chem. Soc. 116 (1994) 8368.
[16] A.R. Dongré, J.L. Jones, Á. Somogyi, V.H. Wysocki, J. Am. Chem. Soc. 118 (1996) 8365.
[17] A.L. McCormack, J.L. Jones, V.H. Wysocki, J. Am. Soc. Mass Spectrom. 3 (1992) 859.
[18] H. Nair, Á. Somogyi, V.H. Wysocki, J. Mass Spectrom. 31 (1996) 1141.
[19] S.J. Gaskell, Biol. Mass Spectrom. 9 (1992) 413.
[20] P.T.M. Kenny, K. Nomoto, R. Orlando, Rapid Commun. Mass Spectrom. 6 (1992) 95.
[21] D. Fabris, K. Michele, M. Constance, Z. Wu, C. Fenselau, J. Am. Soc. Mass Spectrom. 4 (1993) 652.
[22] M.F. Bean, S.A. Carr, G.C. Thorne, M.H. Reilly, S.J. Gaskell, Anal. Chem. 63 (1991) 1473.
[23] X.-J. Tang P. Thibault, R.K. Boyd, Anal. Chem. 65 (1993) 2824.
[24] S.J. Gaskell, M.H. Reilly, Rapid Commun. Mass Spectrom. 2 (1988) 188.
[25] L. Poulter, L.C.E. Taylor, Int. J. Mass Spectrom. Ion Processes 91 (1989) 183.
[26] R.S. Johnson, D. Krylov, K.A. Walsh, J. Mass Spectrom. 30 (1995) 386.
[27] A.R. Dongré, Á. Somogyi, V.H. Wysocki, J. Mass Spectrom. 31 (1996) 339.
[28] S.G. Summerfield, A. Whiting, S.J. Gaskell, Int. J. Mass Spectrom. Ion Process 162 (1997) 149.

[29] S.G. Summerfield, S.J. Gaskell, Int. J. Mass Spectrom. Ion Processes 165/166 (1997) 509.
[30] J. Qin, B.T. Chait, J. Am. Chem. Soc. 117 (1995) 5411.
[31] K.A. Cox, S.J. Gaskell, M. Morris, A. Whiting, J. Am. Soc. Mass Spectrom. 7 (1996) 522.
[32] K.M. Downard, K. Biemann, Int. J. Mass Spectrom. Ion Processes 148 (1995) 191.
[33] J.L. Jones, A. Dongré, H. Nair, Á. Somogyi, V.H. Wysocki, Proceedings of the 43rd ASMS Conference on Mass Spectrometry and Allied Topics, Atlanta, GA, 1995.
[34] O. Burlet, C.-Y. Yang, S.J. Gaskell, J. Am. Soc. Mass Spectrom. 3 (1992) 337.
[35] P.D. Schnier, W.D. Price, R.A. Jockusch, E.R. Williams, J. Am. Chem. Soc. 118 (1996) 7178.
[36] T. Wyttenbach, G.V. Helden, M.T. Bowers, J. Am. Chem. Soc. 118 (1996) 8355.
[37] T. Wyttenbach, J.E. Bushnell, M.T. Bowers, J. Am. Chem. Soc. 120 (1998) 5098.
[38] R.W. Vachet, M.R. Asam, G.L. Glish, J. Am. Chem. Soc. 118 (1996) 6252.
[39] K.D. Ballard, S.J. Gaskell, J. Am. Chem. Soc. 114 (1992) 64.
[40] A.R. Dongré, M.J. Hayward, V.H. Wysocki, Proceedings of the 43rd ASMS Conference on Mass Spectrometry and Allied Topics, Atlanta, GA, 1995.
[41] Q.Y. Wu, S. van Orden, X.H. Cheng, R. Bakhtiar, R.D. Smith, Anal. Chem. 67 (1995) 2498.
[42] G.C. Thorne, K.D. Ballard, S.J. Gaskell, J. Am. Soc. Mass Spectrom. 1 (1990) 249.
[43] G. Tsaprailis, H. Nair, Á. Somogyi, V.H. Wysocki, W. Zhong, J.H. Futrell, S.G. Summerfield, S.J. Gaskell, Proceedings of the 46th ASMS Conference on Mass Spectrometry and Allied Topics, Orlando, FL, 1998.
[44] G. Tsaprailis, H. Nair, Á. Somogyi, V.H. Wysocki, W. Zhong, J.H. Futrell, S.G. Summerfield, S.J. Gaskell, J. Am. Chem. Soc. 121 (1999) 5142.
[45] V.H. Wysocki, A.R. Dongré, in Large Ions: Their Vaporization, Detection and Structural Analysis, T. Baer, C.Y. Ng, I. Powis (Eds.), Wiley, New York, 1996.
[46] V.H. Wysocki, J.-M. Ding, J.L. Jones, J.H. Callahan, F.L. King, J. Am. Soc. Mass Spectrom. 3 (1992) 27.
[47] E.N. Nikolaev, Á. Somogyi, C. Gu, V.H. Wysocki, C. Martin, G.L. Samuelson, R.B. Cody, unpublished.
[48] J.A. Loo, C.G. Edmonds, R.D. Smith, Science 248 (1990) 201.
[49] E. Atherton, R.C. Sheppard, in Solid Phase Peptide Synthesis: A Practical Approach, D. Rickwood, B.D. Hames (Eds.), Oxford University Press, Oxford, UK, 1989.
[50] A. Ulman, Chem. Rev. 96 (1996) 1533.
[51] F. Mohamadi, N.G.J. Richards, W.C. Guida, R. Liskamp, M. Lipton, C. Caufield, G. Chang, T. Henderickson, W.C. Still, J. Comput. Chem. 11 (1990) 440.
[52] P.A. Kollman, J. Am. Chem. Soc. 106 (1984) 795.
[53] E. Polak, G. Ribiere, Rev. Française Inf. Rech. Oper. 16-R1 (1969) 35.
[54] M. Meot-Ner, A.R. Dongré, Á. Somogyi, V.H. Wysocki, Rapid Commun. Mass Spectrom. 9 (1995) 829.
[55] C. Gu, G. Tsaprailis, V. Wysocki, Proceedings of the 47th ASMS Conference on Mass Spectrometry and Allied Topics, Dallas, TX, 1999.
[56] Á. Somogyi, V.H. Wysocki, I. Mayer, J. Am. Soc. Mass Spectrom. 5 (1994) 704.
[57] W. Yu, J.E. Vath, M.C. Huberty, S.A. Martin, Anal. Chem. 65 (1993) 3015.
[58] W.D. van Dongen, H.F.M. Ruijters, H.J. Luinge, W. Heerma, J. Haverkamp, J. Mass Spectrom. 31 (1996) 1156.